

Seeing Through the Trough: Outflows and the Detectability of Ly α Emission from the First Galaxies

Mark Dijkstra^{1*} and J. Stuart B. Wyithe²

¹*Astronomy Department, Harvard University, 60 Garden Street, Cambridge, MA 02138, USA*

²*School of Physics, University of Melbourne, Parkville, Victoria, 3010, Australia*

11 November 2018

ABSTRACT

The next generation of telescopes aim to directly observe the first generation of galaxies that initiated the reionization process in our Universe. The Ly α emission line is robustly predicted to be the most prominent intrinsic spectral feature of these galaxies, making it an ideal target to search for and study high redshift galaxies. Unfortunately the large Gunn-Peterson optical depth of the surrounding neutral intergalactic medium (IGM) is thought to render this line extremely difficult to detect prior to reionization. In this paper we demonstrate that the radiative transfer effects in the interstellar medium (ISM), which cause Ly α flux to emerge from galaxies at frequencies where the Gunn-Peterson optical depth is reduced, can substantially enhance the prospects for detection of the Ly α line at high redshift. In particular, scattering off outflows of interstellar H I gas can modify the Ly α spectral line shape such that $\gtrsim 5\%$ of the emitted Ly α radiation is transmitted directly to the observer, *even through a fully neutral IGM*. It may therefore be possible to directly observe ‘strong’ Ly α emission lines (EW $\gtrsim 50$ Å rest frame) from the highest redshift galaxies that reside in the smallest H II ‘bubbles’ early in the reionization era with JWST. In addition, we show that outflows can boost the fraction of Ly α radiation that is transmitted through the IGM during the latter stages of reionization, and even post-reionization. Coupled with the fact that the first generation of galaxies are thought to have very large intrinsic equivalent Ly α equivalent widths, our results suggest that the search for galaxies in their redshifted Ly α emission line can be competitive with the drop-out technique out to the highest redshifts that can be probed in the JWST era.

Key words: galaxies: high redshift – (galaxies): intergalactic medium – ISM: kinematics and dynamics – line: profiles – scattering – radiative transfer

1 INTRODUCTION

One of the main science drivers of the next generation of telescopes is to detect the first generation of galaxies¹ that formed in our Universe. These galaxies contained hotter and more compact stars (e.g. Tumlinson & Shull 2000; Bromm et al. 2001), whose initial mass function (IMF) was

likely top-heavy (Larson 1998; Bromm et al. 2002). Both the top-heavy IMF and low (or zero) gas metallicity enhanced the number of ionizing photons that the first galaxies emitted compared to that of local galaxies, at a fixed star formation rate (Tumlinson & Shull 2000; Bromm et al. 2001; Schaerer 2002, 2003). This enhancement in ionizing luminosity results in larger H II regions in the interstellar medium (ISM) of these galaxies. As a result, one of the key predicted properties of the first galaxies are prominent nebular emission lines, dominated in flux by hydrogen Ly α ($\lambda = 1216$ Å, see e.g. Johnson et al. 2009). The first generation of galaxies are therefore likely to have been strong Ly α emitters, with equivalent widths possibly as high as EW ~ 1500 Å (Schaerer 2002, 2003; Johnson et al. 2009, also see Partridge & Peebles 1967, Meier 1976).

In this paper we investigate the prospects for detecting this Ly α emission. The first galaxies were surrounded by a mostly neutral intergalactic medium (IGM), which is

* E-mail: mdijkstr@cfa.harvard.edu

¹ The definition of ‘the first generation of galaxies’ is somewhat arbitrary. We take it to mean any star forming galaxy during the earliest stages of the reionization that might be detected (in either their continuum or in on of their lines) by the next generation of telescopes. Although the analysis presented in this paper also applies to the first stars that likely formed one-by-one in minihalos, the overall fluxes from these sources is much too faint to be detected in the near future (regardless of radiative transfer effects that may boost the detectability of Ly α emission from such sources).

extremely optically thick to Ly α radiation. Loeb & Rybicki (1999) showed that scattering of Ly α photons through a neutral IGM causes galaxies to be surrounded by diffuse Ly α halos (also see Kobayashi & Kamaya 2004; Kobayashi et al. 2006). While the total flux in these halos can be substantial, their large angular size results in surface brightness levels that are beyond reach of even future telescopes such as the *James Webb Space Telescope* (JWST, see § 2.1).

If Ly α radiation from the first galaxies is to be detected, it will therefore be via Ly α photons that were transmitted directly to the observer. In a neutral IGM, there are two mechanisms by which this can be achieved:

(i) The first mechanism is due to ionizing radiation that escapes from the galaxy, which creates a surrounding H II ‘bubble’, that can strongly boost the detectability of Ly α emission² (e.g. Haiman 2002; Cen et al. 2005). This is because Hubble expansion redshifts Ly α photons while they propagate freely through the ionized gas. As a result, a fraction of photons enter the neutral intergalactic medium on the red side of the line center, where the IGM optical depth can be smaller by orders of magnitude. For example, the Gunn-Peterson optical depth at redshift z is given by (e.g. Barkana & Loeb 2001)

$$\tau_{\text{GP},0} \approx 7.30 \times 10^5 x_{\text{HI}} \left(\frac{1+z}{10} \right)^{3/2}, \quad (1)$$

where x_{HI} denotes the neutral volume fraction of hydrogen in the IGM. The Gunn-Peterson optical depth (Eq 1) reduces to (Miralda-Escude 1998; Dijkstra & Wyithe 2006)

$$\tau_{\text{GP}}(\Delta v) \approx 2.3 \left(\frac{\Delta v}{600 \text{ km s}^{-1}} \right)^{-1} \left(\frac{1+z}{10} \right)^{3/2} \quad (2)$$

for photons that enter the neutral IGM with a redshift of Δv from line center. Eq 2 illustrates that photons that enter the neutral IGM significantly redward of the Ly α resonance are scattered with only a weak optical depth. However given the high density of the surrounding IGM it is generally assumed that the first galaxies would not have had large enough H II ‘bubbles’ to prevent complete damping of the line.

(ii) The second mechanism for enhancing the transmission of Ly α photons from high redshift galaxies is due to radiative transfer effects within the ISM of galaxies (in particular outflows of interstellar H I gas), which can shift Ly α photons to the red side of the line before it reaches the IGM. Observed interstellar metal absorption lines (Si II, O I, C II, Fe II and Al II) in Lyman Break Galaxies (LBGs) are typically strongly redshifted relative to the galaxies’ systemic velocity (with a median off-set of $\sim 160 \text{ km s}^{-1}$), while the Ly α emission line is strongly redshifted (with a median velocity offset of $\sim 450 \text{ km s}^{-1}$ Steidel et al. 2010, also see Shapley et al. 2003). This suggests that large scale outflows are ubiquitous in LBGs (Shapley et al. 2003; Steidel et al. 2010). Furthermore, scattering of Ly α photons by H I in

² Indeed, the fact that the reionization process likely affects the observed number and distribution of high-redshift Ly α emitting galaxies is exactly the reason why Ly α emitting galaxies are thought to probe this epoch (Haiman & Spaans 1999; Malhotra & Rhoads 2004; Furlanetto et al. 2006; Kashikawa et al. 2006; Dijkstra et al. 2007a; McQuinn et al. 2007; Iliiev et al. 2008; Mesinger & Furlanetto 2008; Dayal et al. 2010).

outflows can successfully explain observed Ly α line shapes in Ly α emitting galaxies at $z = 3-6$ (Verhamme et al. 2006, 2008; Vanzella et al. 2009).

In this paper we explore the outflow mechanism in more detail. We will show that these ‘local’ (i.e. inherent to the galaxy itself) processes in the ISM can cause as much as $\gtrsim 5\%$ of the emitted Ly α radiation to be directly transmitted to the observer *even through a fully neutral IGM*. This result is important for the study of high redshift galaxies, because it suggests that detecting the Ly α emission line of the first generation of galaxies may well be within reach of the next generation of telescopes including JWST.

The outline of this paper is as follows: we describe our models and present our results in § 2. We discuss our models and the implications of this work in § 3, before we conclude in § 4. The cosmological parameter values used throughout our discussion are $(\Omega_m, \Omega_\Lambda, \Omega_b, h) = (0.27, 0.73, 0.046, 0.70)$ (Komatsu et al. 2009).

2 MODELLING OF LY α FROM HIGH REDSHIFT GALAXIES

We divide our study into modelling of three phenomena which are important in the apparent brightness of Ly α emitters at high redshift. Firstly in § 2.1 we compute the integrated (over the sky) flux density, and integrated (over frequency) surface brightness profiles of the Loeb-Rybicki halos that surround the first first generation of galaxies. This calculation illustrates the difficulty of directly detecting these Ly α halos. Then in § 2.2 we show how radiative transfer through a static ISM causes the predicted Loeb-Rybicki halos to be accompanied by Ly α point sources, which are more easily detectable. Finally in § 2.3 we show that this result is strengthened further when the ISM of galaxies contain outflows of H I. In all our calculations we assume that the intrinsic, i.e. the emitted, luminosity of the galaxy is $L_\alpha = 10^{43} \text{ erg s}^{-1}$, which corresponds to a star formation rate of $\text{SFR} \lesssim 2M_\odot \text{ yr}^{-1}$ for $Z \lesssim 10^{-3} Z_\odot$ (Schaerer 2003, for a Salpeter IMF from $1 - 100M_\odot$). For comparison, the brightest observed Ly α sources at $z = 6.5 - 6.6$ have ‘observed’ luminosities (i.e. the observed flux times $4\pi d_L^2(z)$, where $d_L(z)$ denotes the luminosity distance to redshift z) of a few times $10^{43} \text{ erg s}^{-1}$ (Kashikawa et al. 2006; Ouchi et al. 2010). Depending on what fraction of the emitted Ly α flux we detect, their intrinsic luminosities can be significantly higher. Our results scale linearly with L_α .

Throughout this paper, we denote photon frequency with the dimensionless parameter $x = (\nu - \nu_\alpha)/\Delta\nu_\alpha$, in which $\nu_\alpha = 2.47 \times 10^{15} \text{ Hz}$ denotes the Ly α rest-frame frequency; $\Delta\nu_\alpha = \nu_\alpha v_{\text{th}}/c$, $v_{\text{th}} = \sqrt{2k_B T/m_p} = 12.9(T/10^4 \text{ K})^{1/2} \text{ km s}^{-1}$, where T denotes the gas temperature. Here, c , k_B , and m_p denote the speed of light, Boltzmann constant, and the proton mass, respectively. In all our calculations we assume that the gas temperature in the ISM is $T_{\text{ISM}} = 10^4 \text{ K}$, but we have explicitly verified that our final results do not depend on this assumption. Furthermore, the Gunn-Peterson optical depth for photons that enter the IGM while in the red wing of the Ly α line is independent of temperature (see Eq 2), and the assumed IGM temperature of $T_{\text{IGM}} = 300 \text{ K}$ (appropriate for neutral intergalactic gas, see e.g. Pritchard & Loeb 2008) is irrelevant.

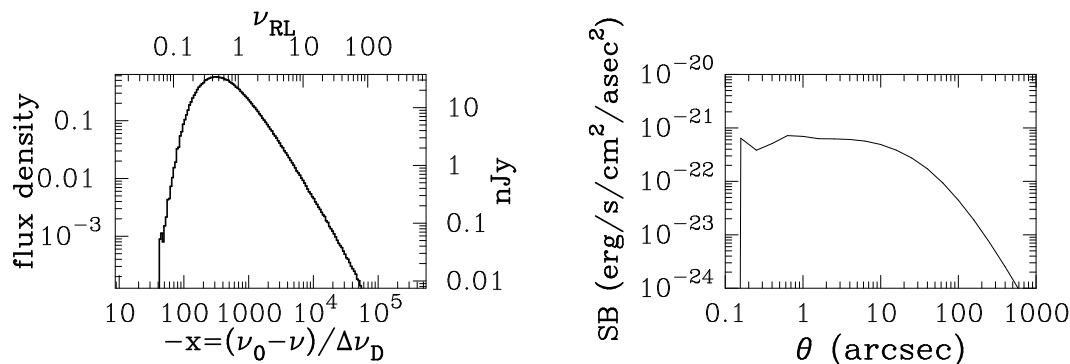


Figure 1. The observed properties of Ly α halos (a.k.a Loeb-Rybicki halos) that surround galaxies embedded within a fully neutral comoving IGM. The ‘noisy’ features in these plots are due to the finite (here $N_{\text{phot}} = 10^6$) number of photons used in our Monte-Carlo calculations. *Left panel:* the *histogram* shows the integrated (over the entire area on the sky) emerging spectrum, under the assumption that all Ly α photons were emitted at line center, and assuming an emitted Ly α luminosity of $L_\alpha = 10^{43}$ erg s⁻¹. The lower horizontal axis shows the dimensionless frequency parameter x , while the upper horizontal axis shows the frequency parameter that was employed by Loeb & Rybicki (1999). The peak flux density occurs at $x \sim -300$ which in our model corresponds to a redshift of ~ 660 km s⁻¹. The FWHM of the spectrum is ~ 1500 km s⁻¹. The vertical axes are expressed in arbitrary units on the left, and physical units on the right. The peak integrated flux density reaches 30 nJy. For comparison NIRSPEC aboard JWST is expected to reach a sensitivity of \sim hundreds of nJy in 10⁴ s ($S/N=10$) for $R=2700$, or line fluxes of $\gtrsim 10^{-19}$ erg s⁻¹ cm⁻². *Right panel:* the integrated (over frequency) surface brightness S as a function of impact parameter (θ) from the galaxy. We find that $S < 10^{-21}$ erg s⁻¹ cm⁻² at all θ . This plot illustrates that it will be extremely difficult to directly detect these Ly α halos (see text).

2.1 Loeb-Rybicki Halos

Figure 1 shows the observed properties of Ly α halos that surround galaxies embedded within a fully neutral comoving IGM. The *histogram* in the *left panel* shows the integrated (over the entire area on the sky) emerging spectrum computed with the Monte-Carlo Ly α radiative transfer code McHammer (Dijkstra et al. 2006). Following previous work, we assumed in this calculation that the Ly α photons were emitted at line center, i.e. $x = 0$. The lower horizontal axis shows the dimensionless frequency parameter x , while the upper horizontal axis shows the frequency parameter that was employed by Loeb & Rybicki (1999). All Ly α photons emerge with a systemic redshift (i.e. $x \ll 0$). The peak flux density occurs at $x \sim -300$ which corresponds to a redshift of ~ 660 km s⁻¹. The Full Width at Half Maximum (FWHM) of the spectrum is ~ 1500 km s⁻¹. The vertical axes contain arbitrary units on the left, and physical units on the right. The peak integrated flux density is ~ 30 nJy.

The *right panel* shows the integrated (over frequency) surface brightness S (in erg s⁻¹ cm⁻² arcsec⁻²) as a function of impact parameter (θ , angular separation) from the galaxy in arcsec. The surface brightness contains a core out to $\theta \sim 20$ arcsec after which it drops steadily. We find that $S < 10^{-21}$ erg s⁻¹ cm⁻² at all θ . For comparison, Rauch et al. (2008) reached a $1-\sigma$ surface brightness limit of $S_{\text{lim}} = 8 \times 10^{-20}$ erg s⁻¹ cm⁻² in a 92 hr long exposure with the ESO VLT-FORS2 instrument, which represent the deepest observations to date. This, when combined with JWST’s proposed sensitivity limit³ to point sources of $\gtrsim 10^{-19}$ erg s⁻¹ cm⁻², implies that it is and will remain extremely difficult to detect these Ly α halos, even with the next generation of telescopes.

³ See <http://www.stsci.edu/jwst/science/sensitivity/>. This estimate assumes $R = 1000$ or $R = 2700$, and assumes an integration time of 10⁵ s.

2.2 Static ISM

In the previous calculation we assumed that all Ly α escaped from the galaxy at the line center. In reality complex radiative transfer effects occur inside the ISM of a galaxy. H I observations show that local galaxies contain H I column densities of $N_{\text{HI}} \sim 10^{19} - 10^{21}$ cm⁻². Such large columns of H I gas can affect the spectrum of Ly α photons as they emerge from the galaxy. Furthermore, we expect column densities of gas in high redshift galaxies to increase as $\propto (1+z)^2$ (see the end of this section for a more quantitative discussion). It is therefore plausible that Ly α photons need to traverse a substantial, i.e. $N_{\text{HI}} > 10^{20}$ cm⁻², column of H I gas before escaping from the galaxy. To estimate the impact of large H I column densities on the detectability of Ly α emission, we turn to analytic solutions for the spectrum of Ly α photons emerging from static, homogeneous, extremely optically thick media. Following the analyses of Harrington (1973) and Neufeld (1990), Dijkstra et al. (2006) computed the Ly α spectrum emerging from a sphere to be

$$J(x) = \frac{\pi^{0.5}}{\sqrt{24}a\tau_0} \left(\frac{x^2}{1 + \cosh \left[\sqrt{\frac{2\pi^3}{27}} \frac{|x^2|}{a\tau_0} \right]} \right), \quad (3)$$

assuming a source of photons in the center of the sphere. Here, $\tau_0 = 5.9 \times 10^6 (N_{\text{HI}}/10^{20} \text{ cm}^{-2})(T_{\text{ISM}}/10^4 \text{ K})^{-1/2}$ denotes the line center optical depth from the center to the edge of the sphere, and $a = 4.7 \times 10^{-4} (T_{\text{ISM}}/10^4 \text{ K})^{-1/2}$ denotes the Voigt parameter. The function $J(x)$ is normalized to $(2\pi)^{-1}$, and its maximum occurs at $x_p \pm 0.9(a_v\tau_0)^{1/3} \sim \pm 13(N_{\text{HI}}/10^{20} \text{ cm}^{-2})^{1/3}(T_{\text{ISM}}/10^4 \text{ K})^{-1/3}$. This dimensionless frequency shift translates to $\Delta v = \pm 160(N_{\text{HI}}/10^{20} \text{ cm}^{-2})^{1/3}(T_{\text{ISM}}/10^4 \text{ K})^{1/6}$ km s⁻¹. The weak temperature dependence ($\propto T^{1/6}$) explains the weak dependence of our results on the assumed ISM temperature. The Ly α spectrum emerging from a semi-infinite slab with

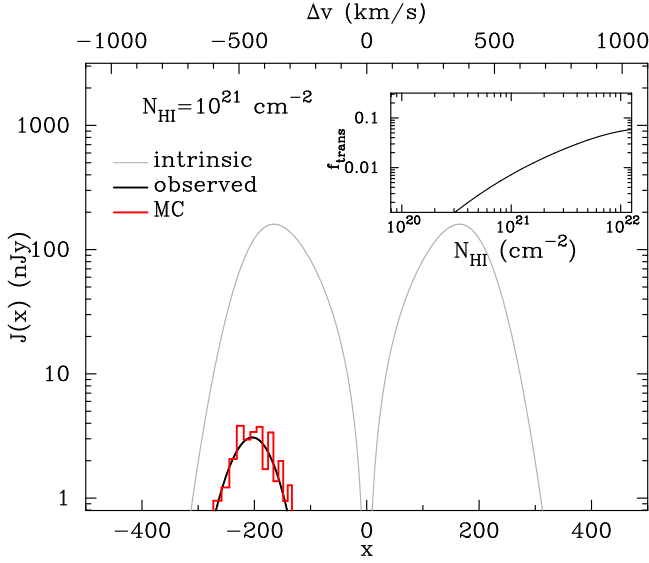


Figure 2. The *solid histogram* in Figure shows the spectrum of Ly α photons that were not scattered at all. These unscattered photons would be observed as a point source. The *grey line* shows the *intrinsic* flux density of the source, $J_{\text{int}}(x)$, which corresponds to the observed Ly α spectrum if we were able to detect all Ly α radiation (Eq 3). Overplotted as the *black solid line* shows the analytic calculation of the observed spectrum $J_{\text{point}}(x)$ given by $J_{\text{int}}(x) \exp(-\tau_{\text{IGM}}[x])$ (see text). The *inset* shows the fraction of directly transmitted Ly α flux, f_{trans} , as a function of H I column density N_{HI} . The transmitted fraction increases from $\sim 1\%$ at $N_{\text{HI}} = 10^{21} \text{ cm}^{-2}$ to $\gtrsim 5\%$ at $N_{\text{HI}} \gtrsim 7 \times 10^{21} \text{ cm}^{-2}$. A transmission f_{trans} of only a few per cent is important: if the intrinsic Ly α EW of the first generation of galaxies was as high as 1500 \AA , then the observed restframe EW is $\text{EW} \sim 50(f_{\text{trans}}/0.03) \text{ \AA}$ (see text)

the same line center optical depth is broader by a factor of 1.1, but is otherwise very similar.

We compute how the predicted properties of the observed Ly α radiation change when we inject photons into a neutral IGM following the distribution given by Eq 3, rather than in the line center (as in § 2.1). The most important difference is that a non-zero fraction of the photons are transmitted directly to the observer without scattering⁴. The *solid histogram* in Figure 2 shows the spectrum of Ly α photons that were not scattered at all. These unscattered photons would be observed as a ‘point source’ (the angular scale is set by the physical scale of the scattering medium), and its peak flux density is $\sim 4 \text{ nJy}$. This peak flux density is smaller than the peak integrated flux density of the Loeb-Rybicki halos, because in this model the total fraction the photons that was transmitted to the observer directly, f_{trans} , was only $\sim 1\%$. For comparison, we have overplotted the *intrinsic* flux density of the source as the *grey line*, as

⁴ The scattered radiation is spread out in a halo that resembles the Loeb-Rybicki halos. However, at small angular separations ($\theta \lesssim 1 \text{ arcsec}$) we find that the surface brightness profile is enhanced by a factor of \sim a few-ten (see Appendix A for an example). This is still well below detection thresholds of existing and future facilities. Furthermore, this enhancement in the central surface brightness profile vanishes when we allow for the existence of an H II region around the galaxy (see Fig A1).

given by Eq 3. This corresponds to the observed Ly α spectrum if we were able to detect all Ly α radiation. Overplotted (*black solid line*) is the analytic calculation of the observed spectrum $J_{\text{point}}(x)$ given by

$$J_{\text{point}}(x) = J(x) \exp(-\tau_{\text{IGM}}[x]), \quad (4)$$

where $J(x)$ is given by Eq 3. Furthermore, $\tau_{\text{IGM}}(x)$ denotes the opacity of the neutral IGM to a Ly α photon that escapes from the galaxy at frequency x , which is $\tau_{\text{IGM}}(x) = \tau_{\text{GP},0} \frac{1}{\sqrt{\pi}} \int_{-\infty}^x \phi(x') dx'$ (e.g. Appendix A of Dijkstra et al. 2006)⁵. Here, $\tau_{\text{GP},0}$ denotes the Gunn-Peterson optical depth given by Eq 1, and $\phi(x)$ denotes the Voigt function (Rybicki & Lightman 1979). Not surprisingly, the analytic calculation agrees well with the Monte-Carlo calculation (which in the end should generate random realizations of this function). We point out that the predicted Ly α spectral line shape is not as asymmetric as is often observed in lower redshift galaxies. This is because the Ly α absorption cross-section varies weakly with frequency (as Δv^{-1} , see Eq 2) in its damping wing, and scattering in the IGM introduces no ‘sharp’ cut-off in the observed Ly α line shape.

The *inset* of Figure 2 shows how the fraction of directly transmitted Ly α flux depends on H I column density N_{HI} . As mentioned previously, $f_{\text{trans}} \sim 10^{-2}$ at $N_{\text{HI}} = 10^{21} \text{ cm}^{-2}$. The transmitted fraction increases to $\gtrsim 5\%$ at $N_{\text{HI}} \gtrsim 7 \times 10^{21} \text{ cm}^{-2}$. For comparison, the central column density for a standard Mo-Mao & White exponential disk—when seen face on—is $N_{\text{HI},0} \sim 3 \times 10^{22} ([1+z]/11)^{3/2} (v_{\text{circ}}/13 \text{ km/s})$, under standard assumptions that the spin parameter $\lambda = 0.05$, and that $j_d = m_d = 0.05$. This suggests that H I column densities in excess of 10^{21} cm^{-2} are expected at the redshifts of interest, and that therefore that f_{trans} can exceed a few per cent.

We stress that although small, a transmission f_{trans} of only a few per cent is important. The total observed flux in the Ly α point source at $z = 10$ is $f_{\text{obs}} = 3.7 \times 10^{-19} (f_{\text{trans}}/0.05) \sim 10^{-19} \text{ erg s}^{-1} \text{ cm}^{-2}$ which is within reach of JWST. For example, an $R = 1000$ grating would yield a $5 - \sigma (f_{\text{trans}}/0.05)$ detection in a 10^5 s exposure (band I). In addition to rendering the line emission from very high redshift galaxies detectable by JWST, this effect could lead to strong Ly α , since given an intrinsic Ly α EW for the first generation of galaxies of $\text{EW}_{\text{int}} = 1500 \text{ \AA}$, the observed restframe EW is $\text{EW} \sim 50(f_{\text{trans}}/0.03) \text{ \AA}$. For comparison, only $\gtrsim 4\%$ of LBGs at $z = 3$ have emission lines with $\text{EW} \gtrsim 50 \text{ \AA}$ (Shapley et al. 2003). Indeed, for an observed rest frame $\text{EW} \sim 75(f_{\text{trans}}/0.05) \text{ \AA}$, and a line flux of $f_{\text{obs}} = 3.7 \times 10^{-19} (f_{\text{trans}}/0.05) \sim 10^{-19} \text{ erg s}^{-1} \text{ cm}^{-2}$

⁵ This implicitly assumes that the gas in IGM is at mean density of the Universe, and that it is co-moving with the Hubble flow. In reality we expect strong departures from the Hubble flow in close proximity to halos, and that the gas is overdense there (Barkana 2004). If we incorporate this into our model, then this increases the opacity of the IGM. However, ionizing radiation that escapes from the galaxy ionizes most of this denser gas. Indeed, we have verified that for escape fractions of ionizing radiation as low as $f_{\text{esc}} = 1\%$, more realistic models of the IGM (as in Dijkstra et al. 2007b) actually transmit more Ly α . The calculations that are present in this paper are therefore conservative.

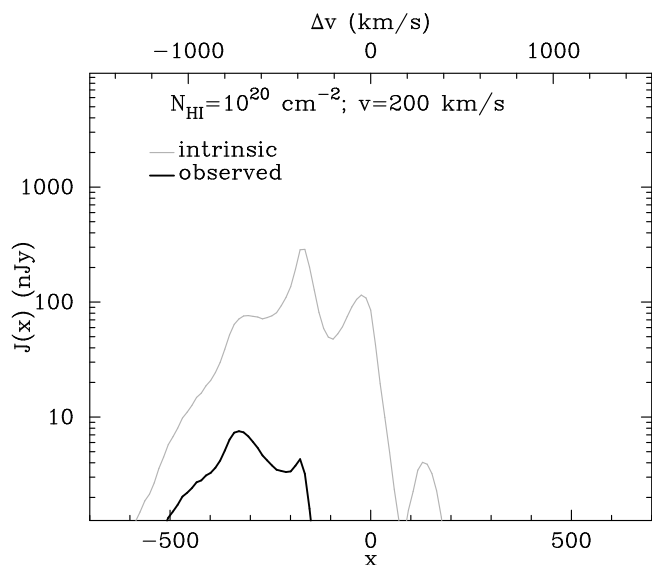


Figure 3. The *black solid line* shows the spectrum of Ly α photons that were transmitted directly to an observer through a fully neutral IGM. The *grey solid line* shows the intrinsic spectrum of this galaxy (see Ahn et al. 2003 and Verhamme et al. 2006 for a detailed discussion on these features in the spectrum). The ISM of this galaxy was modeled as a thin, outflowing (with speed v_{sh}), spherically symmetric shell of H I gas (with column density N_{HI}). This type of model successfully reproduces observed Ly α line shapes in known Ly α emitting galaxies. We assumed that $(N_{\text{HI}}, v_{\text{sh}}) = (10^{20} \text{ cm}^{-2}, 200 \text{ km s}^{-1})$. Because a significant fraction of the radiation comes out of the galaxy with a large systematic redshift, $f_{\text{trans}} \sim 4\%$ of all emitted photons is transmitted directly to the observer.

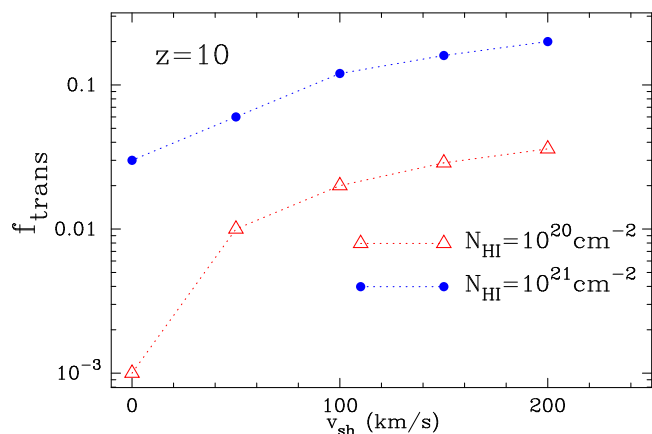


Figure 4. This figure shows the fraction of Ly α photons, f_{trans} , that is transmitted directly through a fully neutral IGM at $z = 10$, as a function of v_{sh} for $N_{\text{HI}} = 10^{20} \text{ cm}^{-2}$ (*red squares*) and $N_{\text{HI}} = 10^{21} \text{ cm}^{-2}$ (*blue squares*). Outflows of $\gtrsim 50 \text{ km s}^{-1}$ can boost f_{trans} tremendously to values as large as $f_{\text{trans}} \sim 10 - 20\%$ (for $v_{\text{sh}} = 200 \text{ km s}^{-1}$). That is, 10 – 20% of all Ly α photons may be transmitted through a fully neutral IGM.

(typical for lower redshift Ly α emitters), the corresponding continuum flux density is $f_{\nu} \sim 2.7 \text{ nJy}$, which would only yield a $\sim 2 - \sigma$ detection in 10^5 s with *NIRCAM* on *JWST*. The Ly α line flux may therefore be (slightly) more easily detectable than the continuum emission, even when we only observe a few per cent of the emitted Ly α flux.

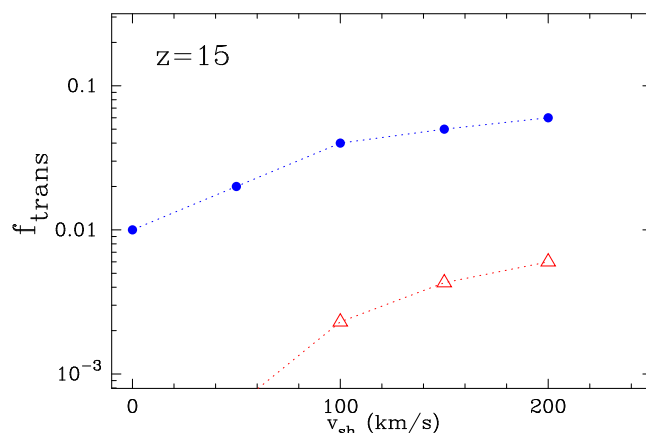


Figure 5. Same as Figure 4, but at $z = 15$.

2.3 Outflowing ISM

Observed galaxies typically show evidence that large scale outflows are ubiquitous in LBGs: interstellar metal absorption lines (Si II, O I, C II, Fe II and Al II) in Lyman Break Galaxies (LBGs) are typically strongly redshifted relative to the galaxies’ systemic velocity (with a median off-set of $\sim 160 \text{ km s}^{-1}$), while the Ly α emission line is strongly redshifted (with a median velocity offset of $\sim 450 \text{ km s}^{-1}$ Steidel et al. 2010, also see Shapley et al. 2003). Scattering of Ly α photons by H I in these outflows has successfully explained observed Ly α line shapes—and their redshifts—in Ly α emitting galaxies at $z = 3 - 6$ (Verhamme et al. 2006, 2008; Vanzella et al. 2009, see § 3.5 for a discussion on this model).

We therefore repeat the exercise of § 2.2 for a suite of outflow models. Following Verhamme et al. (2006, 2008), we model the outflow as a spherically symmetric thin shell of gas that contains an H I column density N_{HI} (also see Ahn et al. 2003), and outflow velocity v_{sh} . We assume that the shell has a radius of 1 kpc and a thickness of 0.1 kpc, but stress that the precise physical scale of the outflow is not important for our results. Our assumed gas temperature in the outflowing H I shell of $T_{\text{ISM}} = 10^4 \text{ K}$ corresponds to a b -parameter of $b \sim 13 \text{ km s}^{-1}$ in the terminology of Verhamme et al. (2008). Our results do not depend on this choice for b , as the amount of flux at large Δv depends very weakly on this parameter (see the *right panel* of Fig 15 of Verhamme et al. 2006). We further assume the H I shells to be dust-free (see § 3.3). Verhamme et al. (2008) typically found that $\log N_{\text{HI}} \sim 19 - 22$, and $v_{\text{sh}} \sim 0 - 500 \text{ km s}^{-1}$, and this is the range of parameter space we explore. We compute Ly α spectra emerging from the outflows with the Monte-Carlo transfer code (Dijkstra et al. 2006). In our calculations, the Ly α photons are emitted at line center, i.e $x = 0$. We verified that our results are insensitive to this assumption⁶. We compute the impact of the IGM on the directly observed

⁶ We repeated some calculations in which Ly α photons were emitted following a Gaussian distribution with a standard deviation of $\sigma = 100 \text{ km s}^{-1}$. While the precise emerging line shapes changed, the overall transmitted fraction remained practically identical.

fraction of Ly α by simply suppressing the intrinsic spectrum by $\exp(-\tau_{\text{IGM}}[x])$ (see § 2.2).

The *grey solid line* in Figure 3 shows an example of the intrinsic spectrum for a model in which we assumed that $(N_{\text{HI}}, v_{\text{sh}}) = (10^{20} \text{ cm}^{-2}, 200 \text{ km s}^{-1})$. The intrinsic spectrum is highly asymmetric, with more flux coming out on the red side of the Ly α line center. The spectrum peaks at about $\sim 2v_{\text{sh}}$, as expected for radiation that scatters back to the observer on the far side of the galaxy (see Verhamme et al. 2006, and Ahn et al. 2003 for a detailed discussion on these features in the spectrum). However, a significant fraction of the radiation comes out at larger redshifts. This radiation can be transmitted directly to an observer through a neutral IGM, and would be observed as a point-source. The *black solid line* shows the spectrum of the point source (see Appendix A for a plot of the surface brightness profile of the scattered radiation). We find that the spectrum of the point source contains $f_{\text{trans}} \sim 4\%$ of all emitted photons. Note that the FWHM of the observed spectrum of the galaxy, as well as the offset arise purely from radiative transfer effects.

The directly transmitted fraction f_{trans} depends on both N_{HI} and v_{sh} . In Figure 4 we show f_{trans} as a function of v_{sh} for $N_{\text{HI}} = 10^{20} \text{ cm}^{-2}$ (*red squares*) and $N_{\text{HI}} = 10^{21} \text{ cm}^{-2}$ (*blue squares*). Having outflows as low as $\gtrsim 50 \text{ km s}^{-1}$ makes a significant difference in the predicted f_{trans} . For example, we find $f_{\text{trans}} \gtrsim 5\%$ for $v_{\text{sh}} \gtrsim 200$ (50) km s^{-1} for $\log N_{\text{HI}} = 20$ ($\log N_{\text{HI}} = 21$). We stress that the outflow parameters were chosen to lie the range required to explain line shapes of observed LAEs at $z < 6$. If the dark matter halos that host the highest redshift galaxies had lower masses (as expected in a hierarchical structure formation scenario), then outflows at higher redshift may have occurred at lower speeds, because of the observed (at lower redshifts) scaling of outflow velocity with circular velocity of the host dark matter halo (e.g. Martin 2005). On the other hand, higher redshift galaxies are expected to be more compact, and therefore we naively expect larger column densities of H I gas at higher redshifts (see § 2.2), in which case low outflow velocities can boost f_{trans} tremendously. The outflow properties in the highest redshift galaxies, and their impact on Ly α propagation is clearly a topic that needs further investigation.

3 DISCUSSION

In this section we discuss a range of issues arising from our model.

3.1 Detecting Ly α Emission During and After the Epoch of Reionization

The results of the previous section focused on the first generation of galaxies that were surrounded by a neutral IGM. However our work applies more broadly. For example, radiative transfer effects in the ISM can also boost the detectability of the Ly α line emitted by galaxies during the later stages, and even post-reionization. It is generally thought that ionized intergalactic gas is transparent to Ly α radiation. More specifically, residual H I that exists inside the ionized IGM is assumed to only affect radiation frequencies that lie blueward of the Ly α resonance. However, in the standard cosmological model (ionized) intergalactic gas

in close proximity to galaxies is expected to be overdense ($1 + \delta \sim 2 - 20$, Barkana 2004). Furthermore, gravity causes this gas to flow towards galaxies. This inflowing, denser ionized gas is expected to scatter a significant fraction of the Ly α photons out of the line of sight. Even the ionized IGM therefore transmits on average as little as $\sim 10 - 30\%$ of the Ly α to an observer (Dijkstra et al. 2007b; Iliev et al. 2008; Zheng et al. 2010a; Dayal et al. 2010). It is therefore unclear whether H II regions during the reionization process actually transmit enough Ly α flux to an observer, to render it detectable.

However in the presence of H I outflows, the transmitted fraction of Ly α radiation through ionized gas can increase dramatically. This is because the outflowing H I gas imparts a redshift to the Ly α photons that is well in excess of \sim a few hundred km s^{-1} (see § 2.3 and Fig 3). On the other hand, the influence of the ionized IGM only extends out to $\Delta v \lesssim v_{\text{infall}}$ (Barkana 2004). Here, the inflow velocity, v_{infall} , is of order the circular velocity of the dark matter halo hosting the galaxy, $v_{\text{infall}} \sim v_{\text{circ}} = 80(M_{\text{halo}}/10^{10} M_{\odot})^{1/3}([1+z]/11)^{1/2} \text{ km s}^{-1}$ (e.g. Barkana & Loeb 2001, where M_{halo} denotes the dark matter halo mass). The impact of the ionized IGM in close proximity to the galaxy is therefore significantly weaker when H I outflows are important in shaping the Ly α spectral line shape that emerges from galaxies.

This implies that winds can have important consequences when interpreting the observed sudden drop in the Ly α luminosity between $z = 6.5$ and $z = 5.7$ (Shimasaku et al. 2006; Kashikawa et al. 2006; Ota et al. 2008, also see Ouchi et al. in prep). The most important aspect of this observation is that the rest-frame UV luminosity function of these same galaxies does not evolve between these redshifts (within the uncertainties, Kashikawa et al. 2006). Indeed, Dijkstra et al. (2007a) have shown that these two observations combined translate to a reduction in the number of detected Ly α photons from $z = 6.5$ by a factor of 1.1–1.8 (95% CL) relative to $z = 5.7$. The simplest interpretation of this observation is that the IGM at $z = 6.5$ is more opaque to Ly α photons than at $z = 5.7$, because the IGM naturally only affects the observed Ly α flux. Dijkstra et al. (2007a) argued that this can be explained quite naturally by an evolution in the opacity of the ionized IGM. However, if winds reduce the impact of the ionized component, then this conclusion becomes uncertain, and the observed reduction in the Ly α luminosity function may be at least partly a reionization-induced signature. In order to understand the evolution of the transmission in terms of the reionization history it is therefore crucial to understand the properties of winds in high-redshift galaxies, and how they affect the transport of Ly α radiation.

3.2 Detecting Other Lines

In this paper we have focused our attention on the Ly α emission line, because it is predicted to be the strongest spectral line of high redshift galaxies. It may be possible to detect other spectral lines as well.

The most prominent alternative emission line is H α ($\lambda = 6563 \text{ \AA}$), which is intrinsically weaker than Ly α in flux by a factor of ~ 8 , under the assumption of case-B recombination. However only a fraction $f_{\text{trans}} = 0.05$ of the emitted Ly α radiation is transmitted, so that the observed H α flux

may be larger by a factor of $\sim 2.5(f_{\text{trans}}/0.05)^{-1}$. On the other hand the H α line lies deeper in the IR, $\lambda = 7([1+z]/11)$ μm , where JWST's *Mid Infrared Instrument* would yield a lower S/N detection of the H α line for medium resolution spectroscopy. This suggests that it may be more difficult to detect H α than naively expected.

In addition the Helium Balmer α (HeII $\lambda = 1640 \text{ \AA}$) line could contain a flux that is comparable to that of H α (Oh et al. 2001; Johnson et al. 2009). However, the predicted strength of this line depends sensitively on the IMF, and it can be weaker than H α by an order of magnitude for reasonable model assumptions (Johnson et al. 2009). On the other hand, the composite spectrum of *observed* $z = 3$ LBGs contains a HeII $\lambda = 1640 \text{ \AA}$ emission line (Shapley et al. 2003). The Full Width at Half Maximum of this line is $\text{FWHM} \sim 1500 \text{ km s}^{-1}$, which is broader than the FWHM of most other nebular emission lines. The origin of this line is not resolved. The line has been associated with population III star formation (Jimenez & Haiman 2006) occurring in pockets of pristine gas that persisted down to low redshift, but may also originate in winds associated with massive Wolf-Rayet stars. In this latter case the line is expected to vanish for low gas metallicities (Brinchmann et al. 2008). Thus it is not clear whether the detection of HeII $\lambda = 1640 \text{ \AA}$ in $z=3$ LBGs implies that this line should be present in the higher redshift galaxies.

Finally, we expect numerous recombination lines associated with metals heavier than Helium (such as [O II], [O III], [S II], ..., e.g. Huchra 1977). Again, robust predictions of the strengths of these lines (which fall in the restframe optical) do not exist as it requires an accurate knowledge of the metallicity of H II regions in high-redshift galaxies.

3.3 Dust

Our calculations have ignored dust. To understand the impact of dust on the Ly α radiation field requires understanding the Ly α transfer process through the ISM of galaxies⁷. This is because the scattering process causes Ly α photons to traverse different paths through the ISM than restframe UV continuum photons (Charlot & Fall 1991; Neufeld 1991; Hansen & Oh 2006; Laursen et al. 2009). As a result dust has a different impact on Ly α line and UV continuum photons. Observations indicate the Ly α escape fraction decreases with the dust content of galaxies. More specifically, the mean Ly α equivalent width decreases with the observed reddening of Lyman Break Galaxies (Shapley et al. 2003). Verhamme et al. (2008) have used their models to quantify the actual escape fraction of Ly α photons from galaxies, $f_{\text{d,esc}}$, as a function of the observed dust reddening, and

found that on average $f_{\text{d,esc}} \sim 10^{-7.7E(B-V)}$. Bouwens et al. (2010) recently argued that candidate galaxies at $z = 7$ are considerably bluer than at lower redshifts. Their most luminous candidates are consistent with $E(B-V) \sim 0.05$, which translates to $f_{\text{d,esc}} \sim 0.4$ (which is significantly higher than Ly α escape fraction inferred for galaxies at $z \lesssim 2$ see e.g. Hayes et al. 2007, 2010). If we take this number literally, then our quoted Ly α fluxes are high by a factor of ~ 2.5 (which implies that dust is not the dominant uncertainty). Moreover, in hierarchical models of galaxy formation, we expect galaxies at higher redshifts, and lower luminosities to be less evolved, and hence the impact of dust is likely to be weaker.

The relation derived by Verhamme et al. (2008) was obtained by averaging over a dozen galaxies, and there exists considerable scatter around their derived relation. For example, observations of low-redshift star forming galaxies with the *International Ultraviolet Explorer* (IUE) and the *Hubble Space Telescope* (HST) revealed very weak Ly α emission (or even strong absorption) in metal poor objects (Hartmann et al. 1984, 1988; Kunth et al. 1994), while strong Ly α emission could be detected from some metal and dust rich galaxies (e.g. Lequeux et al. 1995). This scatter is likely related to the precise geometry of the dust distribution (Scarlata et al. 2009), viewing angle towards the galaxies (Laursen et al. 2009), and outflows. When outflows are present in galaxies, the strength of Ly α emission appears to be independent of the dust content of the galaxy. In the absence of strong outflows however, Ly α line strength appears to decrease with dust content (Kunth et al. 1998; Atek et al. 2008). Our work implies that in high redshift galaxies, H I outflows further affect the subsequent impact of the IGM on the detectability of Ly α emitting galaxies.

3.4 Peculiar Velocities

Following the announcement of the discovery of a $z = 10$ galaxy by Pelló et al. (2004)—which was later disputed (Bremer et al. 2004; Weatherley et al. 2004)—, Cen et al. (2005) argued that the line could be detected through a fully neutral IGM, if the Ly α emitting region in the galaxy was receding relative to the surrounding absorbing IGM with $v \gtrsim 35 \text{ km s}^{-1}$. In this study, the galaxy ionized an H II region with a radius of $\sim 0.28 \text{ pMpc}$. While peculiar velocities of this magnitude do not play an important role in reducing the Gunn-Peterson damping wing optical depth (for which one needs $\Delta v \gtrsim 500 \text{ km s}^{-1}$, Eq 2), they can play a role in reducing the opacity of the ionized ‘local’ IGM (see § 3.1), just like outflows. However, both mechanisms are expected to leave different signatures on the observed Ly α line shape: scattering off H I outflows is expected to result in asymmetric emission lines (see Fig 3), while peculiar velocities may leave an intrinsically symmetric emission line symmetric (Cen et al. 2005). We caution that symmetric Ly α emission lines may be observed as a result of scattering through a static ISM (see Fig 2), but point out that in the latter case the Ly α peak flux density is redshifted by $\sim 500 \text{ km s}^{-1}$ relative to the galaxy’s systemic redshift. This shift is much larger than that expected for the model that uses peculiar velocities, which is $\sim 35 - 70 \text{ km s}^{-1}$.

⁷ Several groups have included dust when modeling the observed number density of Ly α emitters (e.g. Haiman & Spaans 1999; Mao et al. 2007; Kobayashi et al. 2010; Dayal et al. 2010). When comparing such models with actual data, a degeneracy exists between the opacity of the ionized IGM and dust to Ly α radiation (i.e. predicted number densities are not sensitive to what the exact source of opacity is). As argued in this section, understanding how outflows shape the intrinsic Ly α emission line that emerges from galaxies provide such models with important new constraints on the IGM—and therefore—dust opacity.

3.5 Comments on the Model

The model used to generate Ly α line profiles in this paper assumes a single, thin, compact, spherical shell of HI gas surrounding the Ly α source (following Ahn et al. 2003; Verhamme et al. 2006, 2008; Vanzella et al. 2009). Recently, Steidel et al. (2010) described an alternative simple outflow model that folds in constraints from observed profiles of interstellar metal absorption lines. This model can also reproduce observed Ly α line shapes in LBGs. In this model, the outflow can extend out to ~ 100 kpc, and outflow velocity increases with radius. It is not clear whether the models are incompatible: one can imagine the outflow extends over a wide range of velocities and spatial scales, but that the outflow's opacity to Ly α photons is dominated by gas closer to the galaxy that is restricted to a narrower range of velocities. As a result, it is possible to model the impact of the outflow on the Ly α radiation field as a single shell that has a low velocity dispersion. This is clearly an issue that needs further investigation. However, a more detailed investigation is beyond the scope of the present paper, especially because our main results are not likely sensitive to the precise model that one uses to describe the impact of the outflow on the Ly α radiation field.

In detail, the directly transmitted fraction of Ly α photons through the IGM at the highest redshifts (the ‘first’ galaxies at $z > 10$) probably depends quantitatively on the precise outflow model that one uses, since different models may imply different predicted redshift evolution. For example, in the models of Verhamme et al. (2006, 2008) and Vanzella et al. (2009) the emission in the red wing of the line (at $\Delta v \gtrsim 500$ km s $^{-1}$) comes from Ly α photons that scatter back and forth repeatedly between the expanding HI outflow. In the model of Steidel et al. (2010) this frequency ‘diffusion’ does not occur, and the emission in the red wing of the line reflects the maximum velocity in the outflow. In this latter model, the flux in the red wing of the line is suppressed at $z > 10$ if the outflow velocities are much lower at high redshift (see the end of § 2.3). On the other hand, it is difficult to completely suppress frequency diffusion. Significant frequency diffusion occurs even in clumpy outflows with a covering factor of only $f_{\text{cov}} \sim 0.5$ (Hansen & Oh 2006, their Fig 19), which is less than the outflow covering factor inferred by Steidel et al. (2010) over a significant range of radii. We therefore expect that photons likely emerge at $\Delta v \gtrsim 500$ km s $^{-1}$ from the ‘first’ galaxies in both models, but that the fraction of the flux that emerges at these frequencies—and therefore f_{trans} —depends on the detailed properties of the HI in outflows in galaxies at these redshifts. This underlines one of our conclusions presented in § 4 (also see § 3.1), that it is crucial to understand the gas kinematics in the ISM (and/or circumgalactic medium) of high-redshift galaxies in order to infer the properties of the IGM from the observed Ly α flux.

Our main results regarding galaxies during the later stages of—and after—reionization ($z \lesssim 8$) require less (or no) extrapolation to higher redshifts, and practically do not depend at all on the precise underlying model of the Ly α line shape. Instead these results rely only on the fact that the *observed* Ly α line shape can extend to frequencies that lie well beyond $\Delta v \sim 500$ km s $^{-1}$ out to $z = 5.5$ (Vanzella et al. 2009).

It has been argued that radiation pressure on dust grains—which in turn are coupled to the interstellar gas—provide an important source of pressure in the ISM of galaxies, and that the observed outflows in galaxies are driven predominantly by radiation pressure (see e.g. Murray et al. 2005). Given that the highest redshift galaxies likely contained little dust (see § 3.3), radiation pressure may be less important in these galaxies, and outflows could be weakened significantly. Interestingly, especially in these first galaxies, a significant fraction ($\sim 20\%$) of the total bolometric luminosity of the galaxy is Ly α line radiation. If this radiation is ‘trapped’ by a large column of H I gas, then the radiation pressure exerted by this Ly α radiation itself becomes important in driving the H I gas out (Dijkstra & Loeb 2008), thereby enhancing the detectability of the Ly α emission.

4 CONCLUSIONS

The next generation of telescopes aim to directly observe the first generation of galaxies that initiated the reionization of our Universe. The Ly α emission line is robustly predicted to be the most prominent intrinsic spectral feature of these galaxies. In this paper we investigated the prospects for detecting this Ly α emission, taking account of radiative transfer effects that are likely to occur in the interstellar medium (ISM) of these galaxies.

Observed interstellar metal absorption lines (Si II, O I, C II, Fe II and Al II) in Lyman Break Galaxies (LBGs) are typically strongly redshifted relative to the galaxies’ systemic velocity (with a median off-set of ~ 160 km s $^{-1}$), while the Ly α emission line is strongly redshifted (with a median velocity offset of ~ 450 km s $^{-1}$ Steidel et al. 2010, also see Shapley et al. 2003). This suggests that large scale outflows are ubiquitous in LBGs (Shapley et al. 2003; Steidel et al. 2010). Furthermore, scattering of Ly α photons by H I in outflows has successfully explained the observed Ly α line shapes in Ly α emitting galaxies at $z = 3 - 6$ (e.g. Verhamme et al. 2006, 2008; Vanzella et al. 2009). Scattering off outflows of interstellar H I gas can shift Ly α photons to the red side of the line before it reaches the IGM (Fig 3). At these frequencies the Gunn-Peterson optical depth may be reduced to order unity as a result.

In this paper we investigated the detectability of Ly α radiation under the assumption that the outflows observed at low redshift also occur in the highest redshift galaxies. We found that outflows may cause as much as $\gtrsim 5\%$ of the emitted Ly α radiation to be transmitted directly to the observer, even through a fully neutral IGM (§ 2.3). Since the intrinsic (restframe) equivalent width of the Ly α line can be as high as $\text{EW}_{\text{int}} = 1500$ Å for the first generation of galaxies, the observed $\text{EW} = f_{\text{trans}} \text{EW}_{\text{int}} = 75(f_{\text{trans}}/0.05)(\text{EW}_{\text{int}}/1500 \text{ Å})$ Å. For comparison, only 4% of the $z = 3$ LBG population have larger EWs (Shapley et al. 2003). We showed that for $f_{\text{trans}} \gtrsim 3\%$ it may be easier to detect Ly α line emission with NIRSPEC on the *James Webb Space Telescope* (JWST), than continuum radiation with JWST’s NIRCAM in the same integration time. We also note that the next generation of ground-based 30-m telescopes with diffraction limited AO are expected to be more (less) sensitive than JWST at $\lambda \gtrsim 1.3 \mu\text{m}$ for $R \gg 100$ ($R \lesssim 100$) spectroscopy (see Moun-tain et al. 2009, their Fig 2). That is, ground based high-

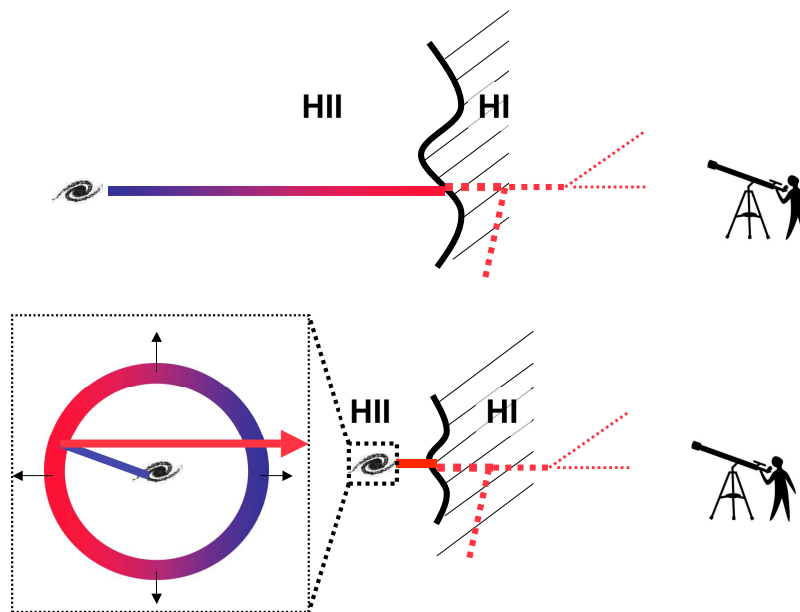


Figure 6. Schematic explanation for why outflows promote the detectability of Ly α emission from galaxies surrounded by significant amounts of neutral intergalactic gas: In the *top panel* a galaxy is surrounded by a large bubble of ionized gas, which in turn is surrounded by neutral intergalactic gas. Ly α emission from this galaxy redshifts away from resonance as it propagates freely through the H II bubble (as indicated by the line color). Once the Ly α photons reach the neutral IGM, they have redshifted far from resonance where the Gunn-Peterson optical depth is reduced tremendously (see Eq 2). Because of the reduced GP optical depth, some fraction of the emitted Ly α is transmitted to the observer without scattering in the IGM. In this drawing, the thickness of the line represents the specific intensity of the Ly α radiation field. The *bottom panel* shows that outflows surrounding star forming regions (represented by the expanding ring. The far side is receding from the observer and has a larger redshift, which is represented by the color) can Doppler boost Ly α photons to frequencies redward of the Ly α resonance. In this scenario, a fraction of Ly α can propagate directly to the observer *without the H II bubble*.

resolution spectroscopic searches for high redshift galaxies can detect fainter galaxies at a fixed integration time when $f_{\text{trans}} \gtrsim 5\%$. Such searches can therefore be competitive with searches that employ the drop-out technique. Irrespective of the survey strategy that is used to search for the highest redshift galaxies, the prospect that Ly α can provide galaxies with spectroscopic redshifts is promising, and important as no robust predictions exists for the detectability of other emission lines (§ 3.2).

This paper has focused on the first generation of galaxies that were surrounded by a neutral IGM, but our work also applies more broadly. For example we argued in § 3.1 that H I outflows promote the detectability of the Ly α emission line during later stages of reionization when much of the absorption is resonant absorption in a highly ionized H II region. As a result outflows can reduce the minimum H II bubble size that is required to render LAEs ‘visible’. This is illustrated schematically in Figure 6. Similarly, H I outflows also promote the detectability of the Ly α emission line after reionization has been completed⁸ (§ 3.1).

In summary, radiative transfer effects in the ISM of high redshift galaxies have been shown to broaden, and—in the case of outflows—redshift the emergent Ly α flux to a level that allows 5% or more of the photons to escape absorption by the neutral IGM. Coupled with the large intrinsic Ly α line EW of the first generation of galaxies, we have shown that searches for galaxies in their redshifted Ly α emission line can be competitive with the drop-out technique out to the highest redshifts that can be probed observationally in the JWST era.

Acknowledgments MD thanks the School of Physics at the University of Melbourne, where most of this work was done, for their kind hospitality. MD is supported by Harvard

⁸ ‘local’ IGM immediately surrounding Ly α sources can introduce a unique anisotropy in the two-point correlation function of LAEs at $z = 5.7$. Zheng et al. (2010b) argued that this scattering-induced signature is reduced when the intrinsic (i.e. prior to scattering) Ly α line width is enhanced. Winds are therefore also expected to reduce this clustering signature. That is, the clustering of LAEs post-reionization can provide constraints on the importance of winds in shaping the Ly α line shape.

⁸ Recently, Zheng et al. (2010b) showed that scattering in the

University funds. We thank Zoltán Haiman & Zheng Zheng for helpful comments on earlier versions of this paper.

REFERENCES

- Ahn, S.-H., Lee, H.-W., & Lee, H. M. 2003, *MNRAS*, 340, 863
- Atek, H., Kunth, D., Hayes, M., Östlin, G., & Mas-Hesse, J. M. 2008, *A&A*, 488, 491
- Barkana, R., & Loeb, A. 2001, *PhR*, 349, 125
- Barkana, R. 2004, *MNRAS*, 347, 59
- Bouwens, R. J., et al. 2010, *ApJL*, 708, L69
- Bremer, M. N., Jensen, J. B., Lehnert, M. D., Schreiber, N. M. F., & Douglas, L. 2004, *ApJL*, 615, L1
- Brinchmann, J., Pettini, M., & Charlot, S. 2008, *MNRAS*, 385, 769
- Bromm, V., Kudritzki, R. P., & Loeb, A. 2001, *ApJ*, 552, 464
- Bromm, V., Coppi, P. S., & Larson, R. B. 2002, *ApJ*, 564, 23
- Cen, R., & Haiman, Z. 2000, *ApJL*, 542, L75
- Cen, R., Haiman, Z., & Mesinger, A. 2005, *ApJ*, 621, 89
- Charlot, S., & Fall, S. M. 1991, *ApJ*, 378, 471
- Dayal, P., Maselli, A., & Ferrara, A. 2010, arXiv:1002.0839
- Dijkstra, M., Haiman, Z., & Spaans, M. 2006, *ApJ*, 649, 14
- Dijkstra, M., & Wyithe, J. S. B. 2006, *MNRAS*, 372, 1575
- Dijkstra, M., Wyithe, J. S. B., & Haiman, Z. 2007a, *MNRAS*, 379, 253
- Dijkstra, M., Lidz, A., & Wyithe, J. S. B. 2007b, *MNRAS*, 377, 1175
- Dijkstra, M., & Loeb, A. 2008, *MNRAS*, 391, 457
- Furlanetto, S. R., Zaldarriaga, M., & Hernquist, L. 2006, *MNRAS*, 365, 1012
- Haiman, Z., & Spaans, M. 1999, *ApJ*, 518, 138
- Haiman, Z. 2002, *ApJL*, 576, L1
- Hansen, M., & Oh, S. P. 2006, *MNRAS*, 367, 979
- Harrington, J. P. 1973, *MNRAS*, 162, 43
- Hartmann, L. W., Huchra, J. P., & Geller, M. J. 1984, *ApJ*, 287, 487
- Hartmann, L. W., Huchra, J. P., Geller, M. J., O'Brien, P., & Wilson, R. 1988, *ApJ*, 326, 101
- Hayes, M., Östlin, G., Atek, H., Kunth, D., Mas-Hesse, J. M., Leitherer, C., Jiménez-Bailón, E., & Adamo, A. 2007, *MNRAS*, 382, 1465
- Hayes, M., et al. 2010, arXiv:1002.4876
- Huchra, J. P. 1977, *ApJ*, 217, 928
- Iliev, I. T., Shapiro, P. R., McDonald, P., Mellema, G., & Pen, U.-L. 2008, *MNRAS*, 391, 63
- Jimenez, R., & Haiman, Z. 2006, *Nature*, 440, 501
- Johnson, J. L. 2009, arXiv:0911.1294
- Johnson, J. L., Greif, T. H., Bromm, V., Klessen, R. S., & Ippolito, J. 2009, *MNRAS*, 399, 37
- Kashikawa, N., et al. 2006, *ApJ*, 648, 7
- Kobayashi, M. A. R., & Kamaya, H. 2004, *ApJ*, 600, 564
- Kobayashi, M. A. R., Kamaya, H., & Yonehara, A. 2006, *ApJ*, 636, 1
- Kobayashi, M. A. R., Totani, T., & Nagashima, M. 2010, *ApJ*, 708, 1119
- Komatsu, E., et al. 2009, *ApJS*, 180, 330
- Kunth, D., Lequeux, J., Sargent, W. L. W., & Viallefond, F. 1994, *A&A*, 282, 709
- Kunth, D., Mas-Hesse, J. M., Terlevich, E., Terlevich, R., Lequeux, J., & Fall, S. M. 1998, *A&A*, 334, 11
- Larson, R. B. 1998, *MNRAS*, 301, 569
- Laursen, P., Sommer-Larsen, J., & Andersen, A. C. 2009, *ApJ*, 704, 1640
- Lequeux, J., Kunth, D., Mas-Hesse, J. M., & Sargent, W. L. W. 1995, *A&A*, 301, 18
- Loeb, A., & Rybicki, G. B. 1999, *ApJ*, 524, 527
- Meier, D. L. 1976, *ApJ*, 207, 343
- Malhotra, S., & Rhoads, J. E. 2004, *ApJL*, 617, L5
- Mao, J., Lapi, A., Granato, G. L., de Zotti, G., & Danese, L. 2007, *ApJ*, 667, 655
- Martin, C. L. 2005, *ApJ*, 621, 227
- McQuinn, M., Hernquist, L., Zaldarriaga, M., & Dutta, S. 2007, *MNRAS*, 381, 75
- Meier, D. L. 1976, *ApJ*, 207, 343
- Mesinger, A., & Furlanetto, S. R. 2008, *MNRAS*, 386, 1990
- Miralda-Escude, J. 1998, *ApJ*, 501, 15
- Mountain, M., et al. 2009, astro2010: The Astronomy and Astrophysics Decadal Survey, 2010, 12
- Murray, N., Quataert, E., & Thompson, T. A. 2005, *ApJ*, 618, 569
- Neufeld, D. A. 1990, *ApJ*, 350, 216
- Neufeld, D. A. 1991, *ApJL*, 370, L85
- Oh, S. P., Haiman, Z., & Rees, M. J. 2001, *ApJ*, 553, 73
- Ota, K., et al. 2008, *ApJ*, 677, 12
- Ouchi, M., et al., to be submitted to *MNRAS*
- Partridge, R. B., & Peebles, P. J. E. 1967, *ApJ*, 147, 868
- Pelló, R., Schaerer, D., Richard, J., Le Borgne, J.-F., & Kneib, J.-P. 2004, *A&A*, 416, L35
- Pritchard, J. R., & Loeb, A. 2008, *Phys Rev D*, 78, 103511
- Rauch, M., et al. 2008, *ApJ*, 681, 856
- Ricotti, M., Gnedin, N. Y., & Shull, J. M. 2008, *ApJ*, 685, 21
- Rybicki, G. B., & Lightman, A. P. 1979, New York, Wiley-Interscience, 1979. 393 p.,
- Scarlata, C., et al. 2009, *ApJL*, 704, L98
- Schaerer, D. 2002, *A&A*, 382, 28
- Schaerer, D. 2003, *A&A*, 397, 527
- Schaerer, D. 2008, *IAU Symposium*, 255, 66
- Shapley, A. E., Steidel, C. C., Pettini, M., & Adelberger, K. L. 2003, *ApJ*, 588, 65
- Shimasaku, K., et al. 2006, *PASJ*, 58, 313
- Steidel, C. C., Erb, D. K., Shapley, A. E., Pettini, M., Reddy, N. A., Bogosavljević, M., Rudie, G. C., & Rakic, O. 2010, arXiv:1003.0679
- Tumlinson, J., & Shull, J. M. 2000, *ApJL*, 528, L65
- Vanzella, E., et al. 2009, arXiv:0912.3007
- Verhamme, A., Schaerer, D., & Maselli, A. 2006, *A&A*, 460, 397
- Verhamme, A., Schaerer, D., Atek, H., & Tapken, C. 2008, *A&A*, 491, 89
- Weatherley, S. J., Warren, S. J., & Babbedge, T. S. R. 2004, *A&A*, 428, L29
- Zheng, Z., Cen, R., Trac, H., & Miralda-Escude, J. 2010a, arXiv:0910.2712
- Zheng, Z., Cen, R., Trac, H., & Miralda-Escude, J. 2010b, submitted to *ApJ*

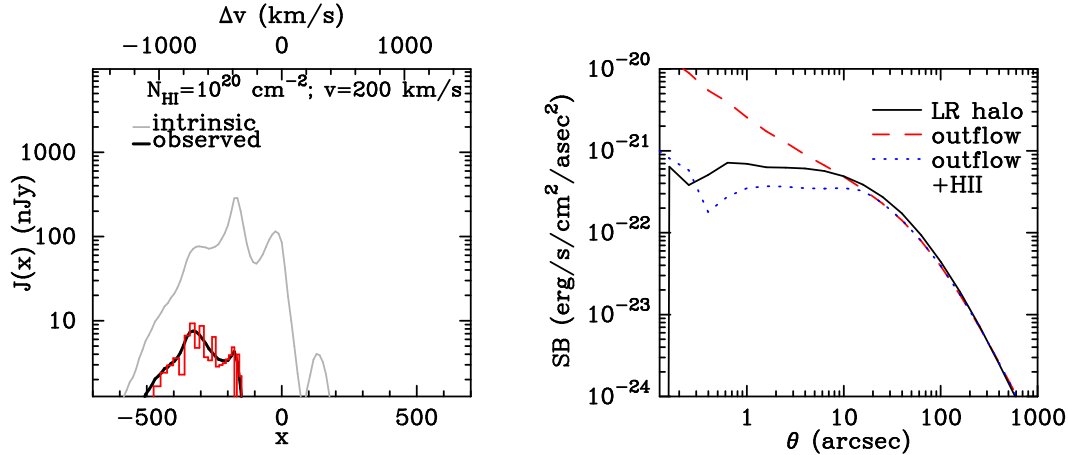


Figure A1. *Left panel:* same as Figure 3. The *red histogram* shows the spectrum of the ‘point source’ (unscattered radiation) as extracted from the Monte-Carlo code. *Right panel:* the *solid black line* shows the surface brightness profile of the standard Loeb-Rybicki halo (scattered radiation, as in Fig 1), while the *red dashed line* shows the surface brightness profile of the scattered radiation for the outflow model. In the outflow model, the surface brightness profile of the Ly α halo is boosted significantly at $\theta \lesssim 5$ arcsec. However, this boost goes away when a small (radius=50 pkpc) is present around the galaxy (as shown by the *blue dotted line*). This figure shows that while outflows boost the detectability of the point source, they do not boost the detectability of the Ly α LR-halos.

APPENDIX A: LOEB-RYBICKI HALOS WITH OUTFLOWS

In the main body of this paper we focused on Ly α radiation that was transmitted directly to the observer through a fully neutral IGM. This radiation is confined to an angular region that is set by the physical scale of the outflow (throughout the paper we referred to this as the ‘point source’), and is much more easily detectable than the scattered Ly α radiation that is in a diffuse halo. For completeness we show how the surface brightness profile of the scattered radiation is modified because of the outflow in the galaxy.

In the *left panel* of Figure A1 the *black solid line* shows the spectrum of unscattered radiation for the model with $(N_{\text{HI}}, v_{\text{sh}}) = (10^{20} \text{ cm}^{-2}, 200 \text{ km s}^{-1})$ (as in Fig 3. The *grey solid line* is again the intrinsic spectrum that emerges from the galaxy). The *red histogram* shows the spectrum of the point source as extracted from the Monte-Carlo code. The agreement between the Monte-Carlo and analytic solution (given by Eq 4) are again good.

In the *right panel* the *black solid line* shows the surface brightness profile of the standard Loeb-Rybicki halo (as in Fig 1), while the *red dashed line* shows the surface brightness profile of the scattered radiation for the outflow model. Clearly, the surface brightness profile is boosted significantly at $\theta \lesssim 5$ arcsec. Radiation that escaped from the galaxy far in the red wing of the line (at $\Delta v \gtrsim 500 \text{ km s}^{-1}$) is most likely to scatter in close proximity to the galaxy, where it is closest to resonance. After this scattering event, these photons again have a non-negligible probability of propagating directly to the observer. This boosts the surface brightness in the inner region of the Ly α halo. We point out that the maximum boost of a factor of ~ 10 is reached at $\theta \lesssim 1$ arcsec. In reality we expect gas to be ionized at such short distances from the galaxy. Indeed, if we insert a small (radius = 50 pkpc) H II bubble around the galaxy, we find that the boost disappears, and we almost recover the original surface brightness profile (as indicated by the *blue dotted line*). Larger H II regions only suppress the surface brightness profile of the central core. The main point of this calculation is to demonstrate that the radiative transfer processes that we invoked to boost the detectability of the ‘point source’ do not also boost the detectability of the Ly α halos.